Gas-Phase Experimental and Theoretical Studies of Adenine, Imidazole, Pyrrole, and Water Non-Covalent Complexes

S. Carles, F. Lecomte, J. P. Schermann, and C. Desfrançois*

Laboratoire de Physique des Lasers UMR CNRS 7538, Institut Galilée, Université Paris-Nord, F-93430 Villetaneuse, France

Received: June 15, 2000; In Final Form: September 12, 2000

We present both experimental and theoretical gas-phase studies of several noncovalent complexes of elementary molecules of biological interest: adenine, imidazole, pyrrole, and water. By means of charge-transfer collisions between those complexes and laser-excited atoms, dipole-bound cluster anions are observed. This Rydberg electron transfer (RET) spectroscopic technique is used to experimentally determine the very weak excess electron binding energies of the complex anions. Theoretical calculations which rely on a homemade semiempirical intermolecular force field allow for the determination of the structures of the low-lying equilibrium configurations of the neutral complexes. The electrostatic properties of these configurations (dipole moments, quadrupole moments, etc.) lead to predicted excess electron binding energies which are compared to the experimental values. This comparison provides a test of the validity of the employed methods, as discussed in the case of the five studied complexes: adenine−imidazole, adenine−pyrrole, adenine−water, pyrrole−water, and imidazole−water.

1. Introduction

Interactions between proteins and nucleic acid bases are of great importance in living systems since they govern the mechanisms of molecular recognition essential for gene expression and control. Most of the knowledge about protein−DNA and protein−RNA complexes has been established by NMR and X-ray diffraction studies but model compounds have been also investigated by means of theoretical[1] and experimental studies conducted in the gas phase.[2] There is currently a large interest in the design of artificial ligands[3,4] which are capable of recognition of unique sites of DNA.[5] Those molecules would specifically bind to sequences of base pairs precisely identified in the deciphered human genome and provide tools for control of gene expression. Among artificial ligands, hairpin polyamides containing pyrrole, 3-hydroxypyrrole, and imidazole can distinguish all four Watson−Crick base pairs in the minor groove of DNA. Molecular modeling studies of those artificial ligands[4] have been performed using force-fields parameters. The starting structures were then derived from NMR structures of large complexes containing imidazole, pyrrole, and poly-desoxynucleosides. A distance-dependent dielectric constant and a layer of water molecules were added in order to mimic biological conditions. As shown by an analysis of protein−nucleic acid base recognition sites, water molecules are indeed nearly always present in those sites and can establish bridges which mediate shape complementarity.[6]

We here employ a very different and more microscopic approach in order to investigate the interactions between pyrrole, imidazole, and adenine. Our aim is to obtain gas-phase experimental data which can be directly compared either to ab initio quantum chemistry calculations or to empirical force fields. To take into account the ubiquitous presence of water in biological systems, we also consider the hydrated complexes of those molecules. We use Rydberg electron transfer (RET) spectroscopy,[7] a method which takes advantage of the rather large polarity of most molecules of biological interest and relies on the determination of dipole moment configurations of the complex by comparison between experimental data and results of semiempirical calculations.[8,9] As compared to usual UV optical spectroscopic techniques in the gas phase,[10−12] this method does not require the presence of a chromophore molecule with a well-defined UV spectroscopy in the complex. However, as discussed below, it requires that the studied complex possesses a large enough polarity together with a negative valence electron affinity. The principle of this method is briefly described in the next section, and the comparison between experimental and theoretical results of the noncovalent complexes of adenine, imidazole, pyrrole, and water is given in Section 3.

2. Rydberg Electron Transfer Spectroscopy

2.1. Method. We will here consider neutral noncovalent complexes of polar molecules which valence electron affinities are negative. This means that, upon attachment of an excess electron, no stable valence negative ions of those complexes can be formed. However, due to the existence of primarily a large enough total permanent electric dipole moment[13] and secondarily of a quadrupole moment and polarizability,[14] a very weakly bound (in the meV range) excess electron can be accommodated by the electrostatic field in a very diffuse orbital (in the nanometer range), mostly located outside the molecular frame. As it has been shown in many previous studies,[15] the formation of a stable so-called dipole-bound (or multipole-bound) anion only releases very little internal energy into the complex, so that fragmentation is very unlikely to occur, even for weakly bound noncovalent complexes. For the same reasons, the structure of the created dipole-bound anion is generally very similar to that of its neutral parent. However, this may not be

* Author to whom correspondence should be addressed at Laboratoire de Physique des Lasers, Institut Galilée, Villetaneuse, 93430, France. Fax: (33) 1 4940 3200. E-mail: desfranc@galilee.univ-paris13.fr.

10.1021/jp002157j CCC: $19.00
Published on Web 10/28/2000

true for some weakly bound noncovalent complexes for which a reorganization of the neutral geometry, with a low energy expense, is possible and leads to a structure of higher dipole moment, more favorable to dipole-bound anion formation.[9,14]

We form these dipole-bound anions by electron transfer collisions between cold molecular complexes and laser-excited Rydberg atoms, in a crossed beam experiment under single-collision conditions. The use of Rydberg electrons allows for a very efficient electron transfer and for the stabilization of the created anions, leading to cold negatively charged species. Another unique feature of this RET technique is that it is selective with respect to the excess electron binding energy in the dipole-bound anion: electron transfer is efficient only if there is an appropriate matching between the initial Rydberg orbital and the final dipole-bound anion orbital. As further described, this will allow us to precisely determine the excess electron binding energy in the created anion. Since this binding energy is highly related to the electrostatic characteristics (dipole, quadrupole, etc.) and thus to the geometry of the complex, we will thus determine which neutral configuration is likely to have given birth to the observed anions.

2.2. Experimental Data and Excess Electron Binding Energies. Experimental data are anion formation rates in charge-exchange collisions between laser-excited Rydberg atoms and the investigated neutral complexes. They are obtained using a RET spectrometer already described in detail elsewhere.[15] Electrons are transferred from laser-excited xenon atoms in Rydberg states (nf) to neutral complexes. The cold neutral cluster beam is produced by flowing typically 2 bar of helium over two successive heated reservoirs. For the production of hydrated complexes, the first reservoir contains water (35 °C) and the second reservoir contains either adenine (200 °C) or imidazole or pyrrole (80 °C). For the production of adenine complexes, imidazole or pyrrole are in the first reservoir while adenine is kept in the second one. The mixture is expanded through a 0.15 mm pulsed nozzle followed by a heated (100 °C) skimmer. The negative ion clusters produced in charge-exchange collisions between the Rydberg atom beam and the neutral cluster beam are mass-analyzed by means of a linear time-of-flight setup. For each detected anion mass, the variation of the formation rates is measured as a function of the principal quantum number n of the Xe(nf) Rydberg atoms involved in the charge-exchange process. Comparison with the production of valence SF_6^- anions due to collisions with a thermal molecular SF_6 beam provides the relative calibration of the Rydberg atoms.

As quoted above, the formation of dipole-bound anions by RET is expected to lead to peaked anion creation rates as a function of the Rydberg quantum number n. As an example, Figure 1 displays such experimental data for the formation of monomer dipole-bound anions of imidazole and adenine. Anion creation rates are clearly peaked around the respective optimum Rydberg quantum numbers $n_{max} = 12$ and $n_{max} = 15$. From these curves, we can obtain the excess electron binding energy values EA_{DB} by two different ways. The first one consists of using a simple empirical relationship between EA_{DB} and n_{max}, which has been verified with a very good precision for many previously studied dipole-bound species:[15,16]

$$EA_{DB} = 23\ \text{eV}/n_{max}^{2.8} \qquad (1)$$

In the case of imidazole and adenine, this leads respectively to $EA_{DB} = 22$ meV and $EA_{DB} = 12$ meV. The second way is to model the RET process within the framework of a simple curve-crossing model[16] into which the only adjustable parameter is EA_{DB}. Fitting the experimental curves then leads to EA_{DB} values as displayed in Figure 1 and which are very similar to the previous ones. Note that no dipole-bound anion is observed either for neat water molecules or for neat pyrrole molecules.

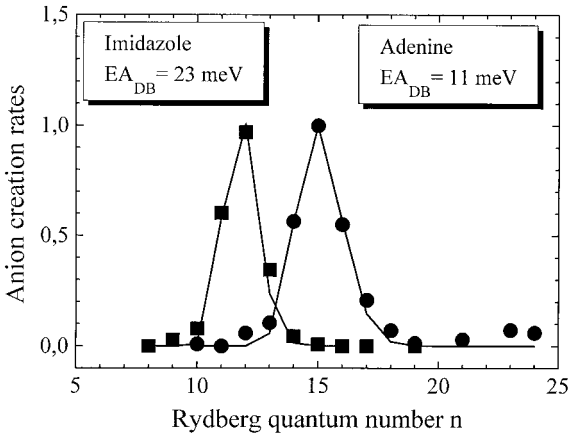

Figure 1. Relative dipole-bound anion formation rates in RET collisions between Rydberg Xe(nf) atoms and adenine (circles) or imidazole (squares) molecules in a supersonic beam. Experimental data are fitted to curve-crossing model calculations which lead to the experimental determination of the excess electron binding energy values, respectively, equal to $EA_{DB}^{exp} = 11$ meV and $EA_{DB}^{exp} = 23$ meV.

2.3. Excess Electron Binding Energies and Molecular Electrostatic Properties. We now need to establish the relationship between the electrostatic properties (dipole, quadrupole, polarizability, etc.) of the neutral molecules or complexes and the excess electron binding energies measured as described above for the observed dipole-bound anions. Quantum chemistry calculations of such loosely bound species are difficult[17,18] and they may be not fully reliable, especially for very loosely bound species. In that case, it is anticipated that a simple semiclassical electrostatic model could be valid since the excess electron lies very far from the neutral core (few nanometers), as in the case of the outer electron of a Rydberg atom for which semiclassical description is valid. We have built such a semiclassical and semiempirical model for dipole-bound (multipole-bound) anions.[14] Its main limitations are that the electron-attaching molecular species is, for simplicity, considered as a symmetric top and that the average distance of the excess electron from the neutral core must be much larger than the spatial extension of the molecular frame, so that the excess electron binding energy is mainly determined by the asymptotic form of the electrostatic interaction potential (dipolar, quadrupolar, polarization). Since it is a semiclassical model, it also takes into account only a fraction of the dispersion interactions, via the static polarizability, between the excess electron and the neutral molecular core.

Despite these limitations, this simple electrostatic model is able to provide rather good estimates of the expected excess electron binding energies for the dipole-bound anions provided that electrostatic characteristics (dipole moment μ, quadrupole moment Q along the μ-direction, and mean polarizability α) are known or calculated. This is especially true for simple molecules as displayed in Table 1 for the monomers considered here. The calculated excess electron binding energy values for dipole-bound anions of adenine and imidazole are in very good agreement with the experimental measurements. For isolated pyrrole and water molecules, the dipole moments (and quadrupole moments) are not large enough to allow for the formation of stable anions, as confirmed by the absence of observed anions. We will see in Section 3 that the predictions of this model may

TABLE 1: Excess Electron Binding Energy Values EA_{DB} for the Four Molecules Studied, As Obtained from Semi-empirical Calculations[14] with the Indicated Electrostatic Parameters and Compared with Experimental Data[a]

molecule	μ (D)	Q (D. Å)	α (Å^3)	EA_{DB}^{calc} (meV)	EA_{DB}^{meas} (meV)
adenine	2.5	15	13.2	12 ± 6	11
imidazole	3.8	−4	7.5	19 ± 4	23
pyrrole	1.74	5	8.0	$<10^{-3}$	
water	1.86	0	1.45	<0	

[a] Dipole moments μ are experimental values from the literature.[29,30] Quadrupole moments Q along the dipole axis are deduced from molecular point charge distributions which reproduce the experimental dipole moment values. Mean polarizabilities α are either experimental values from the literature[29] or estimates from standard bond polarizabilities.

be less good for noncovalent complexes but are reliable enough to validate the comparison between experimental excess electron binding energies and calculated neutral geometry.

3. Comparison between Theoretical and Experimental Results

3.1. Semiempirical Calculations of the Noncovalent Complex Structures. For all complexes studied, we now compare experimental data obtained from RET spectroscopy, as described in the previous section, with calculated equilibrium geometry of lowest interaction potential energies between the two molecules considered. We thus must explore as totally as possible the multidimensional intermolecular potential surface for locating the different possible equilibrium structures and their corresponding dissociation energies D_e. We estimate a temperature for intermolecular degrees of freedom of neutral complexes in our supersonic beam in the collision region, of about 150 K.[8] We will thus not retain all equilibrium configurations which lie higher than about 50 meV above the lowest equilibrium structure, since they are very unlikely to be present in the neutral beam. For each of all other low-lying complex configurations, we then must calculate the total dipole moment, quadrupole moment, and polarizability in order to determine which neutral configuration can give birth to the observed dipole-bound anions and the measured excess electron binding energies and which ones cannot.

Since we wish to explore the intermolecular phase space as extensively as possible, we need a simple analytical and semiempirical model of the intermolecular potential energies. Because we want to calculate accurate dipole and quadrupole moments of the equilibrium configuration, we also need a molecular charge description which respects the actual electrostatic properties of each molecular subunit. Finally, because we have to ascertain the ordering of the different low-lying configurations, we look for intermolecular dissociation energies as accurate as possible. In a large majority of the available force fields, molecular dipole moments are most often overestimated, as a result of the lack of specific hydrogen bond terms and polarization terms. The atomic charges are then artificially increased in order to compensate by Coulombic interactions this lack of interaction energy terms. This lead us to develop our own semiempirical model which fulfills the above conditions and which we have already briefly described.[19] It mainly follows the lines of the work of Scheraga[20] and it will be described in more details elsewhere.[21] The intermolecular potential energy is described in atom−atom Coulombic terms, between partial atomic charges, atom−atom van der Waals terms, specific hydrogen bond terms for the relevant atoms, and static polarization terms on each atom. The crucial ingredients of this model are the partial atomic charges and the hydrogen bond parameters. Partial atomic charges are mainly determined from standard bond dipole moments and are adjusted in order to reproduce the experimental values of the dipole and/or quadrupole moments when they are available for the considered isolated molecules. Hydrogen bond parameters are determined by fitting the available intermolecular interaction energies of model complexes provided either by ab initio calculations or by experimental data. It is clear that this type of semiempirical force field calculation is not expected to lead to fully accurate theoretical data but, as shown in this work and many others, it is an efficient first-order way to interpret experimental results, especially for rather large molecular complexes for which high-level quantum calculations are prohibitive.

The exploration of the intermolecular phase space is performed with the help of a combination of a genetic algorithm[22,23] and of a local minimization method. To be sure that we do not miss any low-lying configuration, we run the genetic algorithm several times with different parameters (rates of mutation, type of reproduction, degree of convergence, size of the phase space, etc.) and we check that no new minimum appears. Low-lying minima (within about 50 meV from the lowest one) are then sorted out according to their intermolecular dissociation energy and we calculate their total dipole moment (including the induced dipole moment contribution) and quadrupole moment from the charge distribution at the equilibrium geometry. The total mean polarizability is simply taken as the sum of the molecular polarizabilities. Using these electrostatic properties, we are thus able to calculate a prediction of the excess electron binding energy in the corresponding dipole-bound anion, as described in Section 2.3 above. For each calculated low-lying equilibrium configuration, these predictions, displayed in Table 2, are then compared to the experimental results, as discussed now.

TABLE 2: Energetic and Electrostatic Characteristics of the Calculated Low-Lying Equilibrium Configurations of the Complexes Studied[a]

complex	D_e (meV)	prob.	μ (D)	Q (D Å)	EA_{DB}^{calc} (meV)	EA_{DB}^{exp} (meV)
adenine−imidazole						55 ± 5
conf. A	360	81%	4.1	44	80 ± 20	
conf. B	335	14%	5.3	48	160 ± 40	
conf. C	320	5%	6.5	48	260 ± 50	
adenine−pyrrole						$60 \pm 5/23 \pm 3$
conf. A	280	53%	1.3	13	<0.5	
conf. B	275	36%	1.7	13	1.5 ± 1	
conf. C	260	11%	4.1	17	55 ± 15	
adenine−water						not observed
conf. A	315	92%	1.1	1	<0	
conf. B	285	8%	4.4	27	85 ± 20	
pyrrole−water						73 ± 5
conf. A	260	99.9%	4.4	24	75 ± 15	
conf. B	175	0.1%	3.0	0	9 ± 3	
imidazole−water						55 ± 25
conf. A	335	94%	6.3	−16	135 ± 20	
			4.7*		50 ± 10	
conf. B	295	5%	6.2	7	190 ± 30	
conf. C	270	1%	5.0	0	115 ± 25	

[a] For each configuration we give the intermolecular dissociation energy D_e, the estimated probability of presence in our supersonic beam (evaluated from a simple Boltzmann law at $T = 150$ K), the total dipole moment μ, and the total quadrupole moment Q along the dipole axis and the corresponding calculated prediction of the excess electron binding energy EA_{DB}^{calc} for the corresponding dipole-bound species. These values have to be compared with the experimental ones EA_{DB}^{exp}, as discussed in the text.

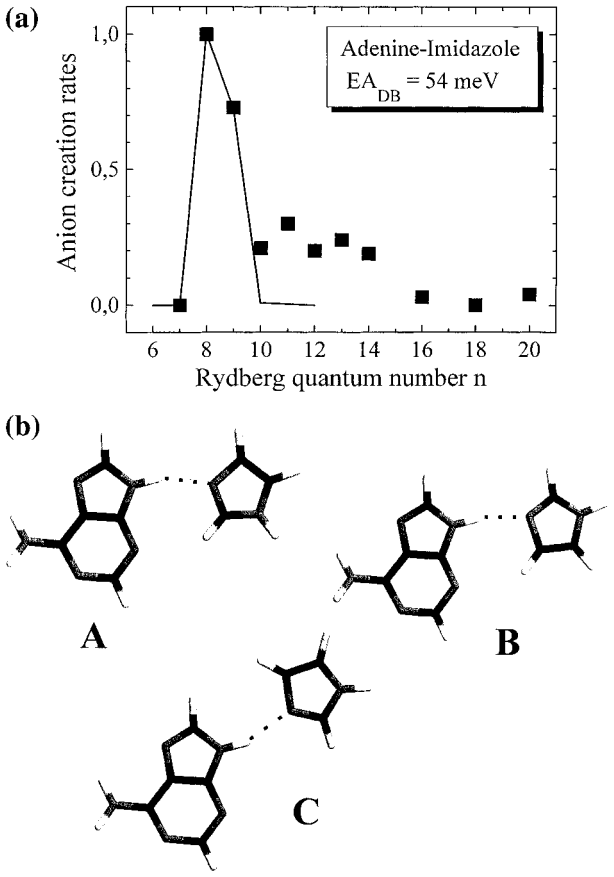

Figure 2. (a) Relative dipole-bound anion formation rates in RET collisions between Rydberg Xe(nf) atoms and adenine−imidazole complexes produced in a supersonic beam. Experimental data are fitted to the curve-crossing model calculations which lead to the experimental determination of the excess electron binding energy value EA_{DB}^{exp} = 55 meV. (b) Structures of the low-lying equilibrium configurations of the adenine−imidazole neutral complexes, as obtained from semiempirical calculations. See text and Table 2 for the labeling and properties.

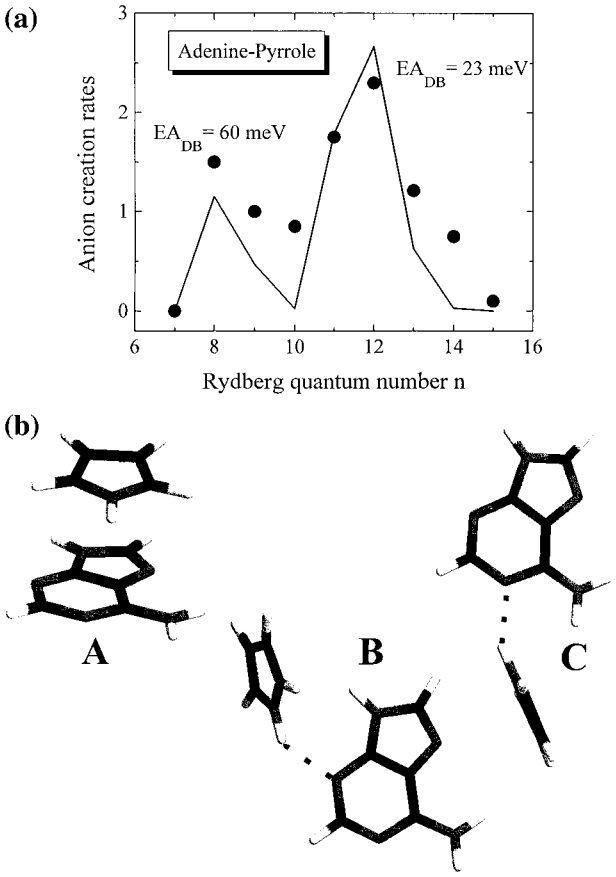

Figure 3. (a) Same as Figure 2a for adenine−pyrrole complexes. The experimental excess electron binding energy values are EA_{DB}^{exp} = 60 meV and EA_{DB}^{exp} = 23 meV. (b) Same as Figure 2b for equilibrium configurations of neutral adenine−pyrrole complexes.

3.2. Adenine−Imidazole. Figure 2a displays the dipole-bound anion formation rates as a function of the Rydberg atom quantum number n involved in the RET collision. There is mainly one peak centered around n_{max} = 8−9 and the empirical relation (eq 1) or the curve-crossing fit gives the corresponding excess electron binding energy EA_{DB}^{exp} = 55 ± 5 meV. In parallel, semiempirical calculations lead to three low-lying equilibrium structures which are drawn in Figure 2b. They both correspond to coplanar structures with a hydrogen bond between the N(9)−H bond of the five-member ring of adenine and the N(1) atom of imidazole (H···N distance of 2.1 Å). In the lowest configuration A, there is a supplementary electrostatic interaction between the N(3) atom of the six-member ring of adenine and the C(2)−H bond located between the N(1) and N(3)−H atoms of imidazole, leading to a total dipole moment of 4.1 D and to a high intermolecular dissociation energy D_e = 360 meV. Lying 25 meV above in energy, there is a second configuration B which is rather similar except that the imidazole molecule is now oriented so that the electrostatic interaction occurs with its C(5)−H bond. The dipole moment increases up to 5.3 D. The third configuration C is located 40 meV above A and the additional electrostatic interaction now occurs between the C(8)−H bond of the five member ring of adenine and the C(5)−H bond of imidazole. The total dipole moment still increases to 6.5 D and both configurations possess high positive quadrupole moment components along the dipole axis. The corresponding predicted excess electron binding energies are thus rather high and, respectively, amount to 80 ± 20, 165 ± 35, and 260 ± 50 meV for configurations A, B, and C. Even if for such rather large values our semiclassical model may not be valid, the two last values seem much too large to correspond to the experimental value. We thus conclude that we indeed observed the formation of dipole-bound anions from complexes with the lowest calculated equilibrium structure A. Furthermore, ab initio calculations[24] have confirmed the present calculated geometry and dipole moment of the lowest configuration A.

3.3. Adenine−Pyrrole. Figure 3a displays the n-dependency of the dipole-bound anion formation rates for adenine−pyrrole complexes. It exhibits a first peak around n_{max} = 8 which is followed by a second peak around n_{max} = 11−12. The empirical relation (eq 1) or the curve-crossing fit give the respective excess electron binding energies EA_{DB}^{exp} = 60 ± 5 meV and EA_{DB}^{exp} = 20−25 meV. On the other side, semiempirical calculations lead to three very different low-lying equilibrium structures which are drawn in Figure 3b. The lowest configuration corresponds to a stacking interaction between the two molecules into which the imidazole molecule interacts with both adenine rings and with a specific interaction between its N(1)−H bond and the N(1) atom of adenine (H···N distance of 3.0 Å). The intermolecular dissociation energy, D_e = 280 meV, is much lower than in the case of adenine−imidazole. The next configuration B, located only about 5 meV above, is very different since the two molecules are now interacting principally through a hydrogen bond between the N(3) atom of adenine and the N−H bond of imidazole (N...H distance of 2.2 Å) and secondarily through an electrostatic interaction between the N(9)−H bond of adenine and the N atom of imidazole (H···N

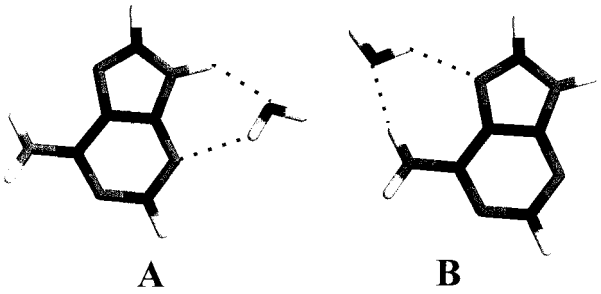

Figure 4. Same as Figure 2b for equilibrium configurations of neutral adenine−water complexes.

distance of 2.6 Å). Both A and B configurations, respectively, possess weak total dipole moments of 1.3 and 1.7 D and moderate positive quadrupole moments along the dipole axis (+13 D Å). The respective calculated excess electron binding energies are thus very low: $EA_{DB}^{calc} < 0.5$ meV and $EA_{DB}^{calc} = 0.5-2.5$ meV. These two configurations probably possess some flexibility, leading to slightly different geometries and dipole moments, but it seems very unlikely that they could be able to give birth to a rather strongly bound dipole-bound species as experimentally observed. On the contrary, the third configuration C, located 20 meV above A, possesses a rather high total dipole moment of 4.1 D, together with a positive quadrupole moment component of +17 D. Å, which leads to a calculated value $EA_{DB}^{calc} = 55 \pm 15$ meV in very good agreement with the largest experimental value. In the corresponding equilibrium geometry, the two molecules are perpendicular and interacts mainly through a hydrogen bond between the N(1) atom of adenine and the N−H bond of pyrrole (N···H distance of 2.1 Å), with a secondary interaction between the H atom of the amino group of adenine and the N atom of pyrrole (H···N distance of 2.6 Å). This third configuration should have a rather small probability of being formed in our supersonic beam (about 11% as estimated from a simple Boltzmann law at $T = 150$ K) thus explaining the relative weakness of the observed anion signals. On the other hand, we did not obtained any low-lying configuration which could account for the observed feature at $n_{max} = 11-12$. More experimental studies, to ascertain the dipole-bound nature of this second peak, and further theoretical calculations, with ab initio methods, may reveal an explanation to this apparent discrepancy between experimental and theoretical data.

3.4. Adenine−Water. As already reported before,[19] we did not observe any dipole-bound anion signal for adenine−water complexes. This should mean that there is no low-lying equilibrium structure of this complex with large enough total dipole moment. From semiempirical calculations, we obtain two low-lying equilibrium configurations into which the water molecule is bound by two hydrogen bonds in the plane of the adenine molecule (see Figure 4). The lowest energy structure[25] A possesses a total dipole moment of 1.1 D and a high intermolecular dissociation energy $D_e = 315$ meV, corresponding to the double hydrogen bond N(9)−H...OH−H···N(3). The second structure B lies 30 meV above but possesses a larger total dipole moment of 4.4 D because the water molecule switch to the other side of the water molecule and forms a double HNH···OH−H···N(7) hydrogen bond. These two structures, with very similar geometry, dipole moments, and relative energies, have also been found in ab initio calculations.[24] The semiclassical model predicts no stable dipole-bound anion for structure A but a rather high excess electron binding energy of $EA_{DB}^{calc} = 85 \pm 20$ meV for structure B. Since this configuration is expected to be nonnegligibly formed in our beam (8%), we should have observed it at low Rydberg quantum numbers.

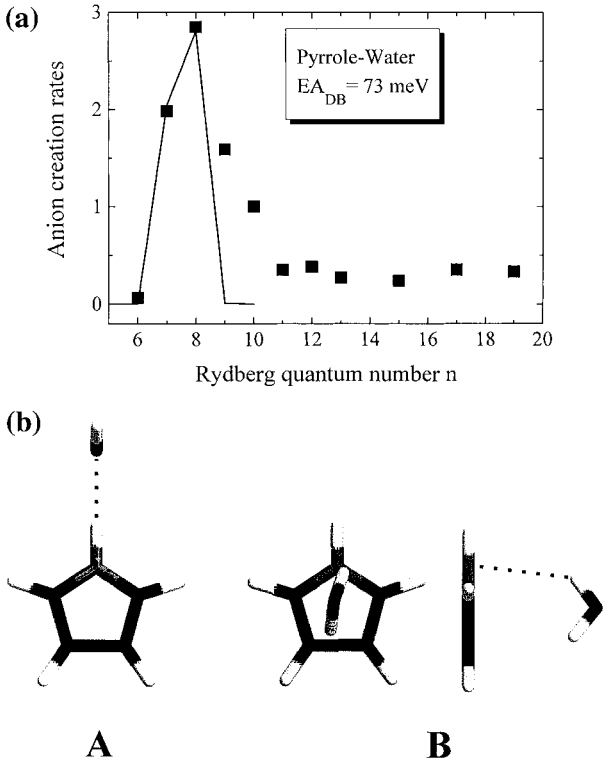

Figure 5. (a) Same as Figure 2a for pyrrole−water complexes. The experimental excess electron binding energy value is $EA_{DB}^{exp} = 73$ meV. (b) Same as Figure 2b for equilibrium configurations of neutral pyrrole−water complexes.

3.5. Pyrrole−Water. Figure 5a displays the *n*-dependency of the dipole-bound anion formation rates for pyrrole−water complexes, and there is a single peak centered around $n_{max} = 7-8$. The empirical relation (eq 1) and the curve-crossing fit provide the excess electron binding energy $EA_{DB}^{exp} = 73 \pm 5$ meV. Semiempirical calculations lead mainly to only one low-lying equilibrium structure A (see Figure 5b) which corresponds to a hydrogen bond between the N−H bond of pyrrole and the water molecule which hydrogen atoms are symmetric with respect to common pyrrole−oxygen atom plane. The intermolecular dissociation energy, $D_e = 260$ meV, is typical of a strong hydrogen bond and the two molecular dipole moments are almost aligned, leading to a total dipole moment (4.4 D) larger than the sum of the individual components (3.6 D) due to the induced effects. The predicted excess electron binding energy is $EA_{DB}^{calc} = 75 \pm 15$ meV, in very good agreement with the experimental value. Previous ab initio calculations[26] also found the same minimum with very similar intermolecular dissociation energy ($D_e = 250$ meV) and total dipole moment (4.8 D). It makes thus no doubt that the observed dipole-bound anions correspond to this configuration. Furthermore, the only other found equilibrium structure (B) is located more than 80 meV above configuration A and is very unlikely to be populated in the beam (see Table 2 and Figure 5b).

3.6. Imidazole−Water. Figure 6a displays the dipole-bound anion formation rates for imidazole−water complexes, as a function of the Rydberg quantum number *n* in the RET collisions. There is one relatively large peak from $n = 7$ to $n = 10$. Furthermore, the anion creation rates do not fall to zero at higher *n*-values but are rather constant at about half that at maximum. The empirical relation (eq 1), with $n_{max} = 8-9$, and the curve-crossing fit give the excess electron binding energy

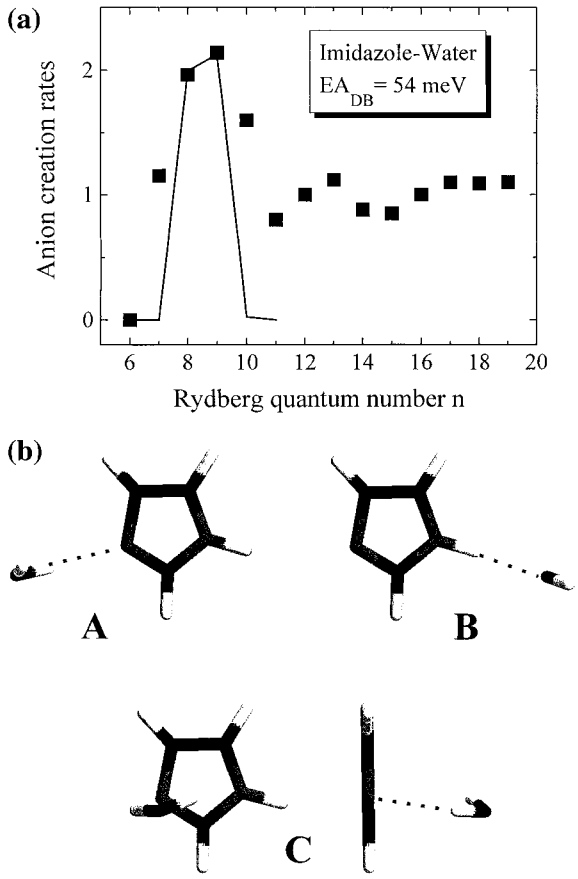

Figure 6. (a) Same as Figure 2a for imidazole−water complexes. The experimental excess electron binding energy value is $EA_{DB}^{exp} = 54$ meV. (b) Same as Figure 2b for equilibrium configurations of neutral imidazole−water complexes.

$EA_{DB}^{exp} = 55 \pm 25$ meV, the large uncertainty being due to the broadness of the peak. On the theoretical side, semiempirical calculations lead to three low-lying equilibrium structures (see Figure 6b) having very different geometries but which both possess large dipole moments. The lowest energy configuration A corresponds to a bent hydrogen bond between the water molecule and the N(1) atom of imidazole, with a high dissociation energy of $D_e = 335$ meV. In the present calculations, the two molecular dipole moments are almost aligned and the resulting total dipole moment is 6.3 D, much larger than the sum of the two individual values (5.6 D). On the other hand, previous ab initio calculations[27] have been reported into which the lowest energy configuration is similar to the present structure A, but with a slightly lower dissociation energy of $D_e = 305$ meV, and with a more linear hydrogen bond, where the oxygen atom is located more in the plane of the imidazole molecule, leading to a lower total dipole moment of 4.7 D. As in the present work for the next structure B, it has been also reported a second equilibrium structure very similar to that of structure A for pyrrole−water, i.e., a symmetric hydrogen bond between the N(3)−H bond of imidazole and the water molecule. The reported total dipole moment of 6.2 D is the same as that calculated here and corresponds to a maximal value obtained from the sum of the individual components and the induced contributions. The only difference is that the relative energy of this second lowest configuration B is here calculated to be equal to 35 meV while it was reported to be only 15 meV in the previous ab initio studies. It is most likely that the present semiempirical calculations underestimate the energy barrier for bending of the hydrogen bond in structure A, leading to a too high dissociation energy and a too high total dipole moment as compared to ab initio results. This is strongly suggested by the comparison to the present experimental results. The predicted excess electron binding energies for structures A and B, deduced from the calculated semiempirical dipole and quadrupole moments, are, respectively, equal to $EA_{DB}^{calc} = 135 \pm 20$ meV and $EA_{DB}^{calc} = 190 \pm 30$ meV, much larger than the experimental result. On the other hand, the predicted value for structure A with the ab initio dipole moment value of 4.7 D becomes $EA_{DB}^{calc} = 50 \pm 10$ meV, i.e., very close to the experimental value. We thus conclude that the observed dipole-bound anions indeed result from electron attachment to the lowest neutral calculated configuration A, but in a linear hydrogen bond geometry as obtained in previous ab initio calculations.[27] Finally, we note that our calculations also give a third equilibrium configuration C in which the water molecule is bridged over the two nitrogen atoms of imidazole (H···N(1) distance of 2.4 Å and H···N(3)H distance of 3.0 Å). However, this structure is located more than 60 meV above A and its dissociation energy may be still overestimated since it also corresponds to very bent hydrogen bonds.

4. Conclusion

The present comparison between model calculations, using semiempirical intermolecular potentials, and experimental studies, performed by means of the RET spectroscopic method of dipole-bound anion formation, on several complexes of elementary molecules of biological interest appears to be very efficient in order to ascertain the validity of the calculated equilibrium structures of the neutral species. It has been shown that our semiempirical force field, associated with a genetic algorithm and a local minimization method, offers a fast means of exploration of the intermolecular phase space and that it generally leads to satisfying energetic and structural results, as compared to either experimental or ab initio calculation results. As illustrated in the case of the imidazole−water complexes, some problems, however, remain concerning the orientation of the hydrogen bonds. Also in the case of adenine−pyrrole complexes, one RET spectral feature has not been assigned, illustrating the need for further experimental or theoretical tools in order to fully understand the exact nature of the observed dipole-bound anions. It is possible to improve the present RET spectroscopic technique of dipole-bound anions by combining it with infrared depletion techniques[12,28] of neutral parent complexes. This would allows for a more direct determination, with a complementary optical spectroscopic technique, of the existence and the nature of the hydrogen bonds in polar complexes.

References and Notes

(1) Saenger, W. *Principles of Nucleic Acid Structure*; Springer-Verlag: New York, 1984.

(2) Galetich, I.; Kosevich, M.; Shelkovsky, V.; Stepanian, S. G.; Blagoi, Y. P.; Adamowicz, L. *J. Mol. Struct.* **1999**, *478*, 155.

(3) White, S.; Szewczyk, J. W.; Turner, J. M.; Baird, E. E.; Dervan, P. B. *Nature* **1998**, *391*, 468.

(4) Tao, Z.; Fujiwara, T.; Saito, I.; Sugiyama, H. *J. Am. Chem. Soc.* **1999**, *121*, 4961.

(5) Hélène, C. *Nature* **1998**, *391*, 436.

(6) Nagy, P. I.; Alagona, G.; Ghio, C. *J. Am. Chem. Soc.* **1999**, *121*, 4804.

(7) Desfrançois, C.; Abdoul-Carime, H.; Schulz, C. P.; Schermann, J. P. *Science* **1995**, *269*, 1707.

(8) Desfrançois, C.; Abdoul-Carime, H.; Khelifa, N.; Schermann, J. P.; Brenner, V.; Millié, P. *J. Chem. Phys.* **1995**, *102*, 4952.

(9) Carles, S.; Desfrançois, C.; Schermann, J. P.; Smith, D. M. A.; Adamowicz, L. *J. Chem. Phys.* **2000**, *112*, 3726.

(10) Courty, A.; Mons, M.; Calvé, J. L.; Piuzzi, F.; Dimicoli, I. *J. Phys. Chem.* **1997**, *101*, 1445.
(11) Nir, E.; Grace, L.; Brauer, B.; Vries, M. S. d. *J. Am. Chem. Soc.* **1999**, *121*, 4896.
(12) Carney, J. R.; Hagemeister, F. C.; Zwier, T. S. *J. Chem. Phys.* **1998**, *108*, 3379.
(13) Desfrançois, C.; Abdoul-Carime, H.; Khelifa, N.; Schermann, J. P. *Phys. Rev. Lett.* **1994**, *73*, 2436.
(14) Abdoul-Carime, H.; Desfrançois, C. *Eur. Phys. J. D* **1998**, *2*, 149.
(15) Desfrançois, C.; Abdoul-Carime, H.; Schermann, J. P. *Int. J. Modern Phys.* **1996**, *10*, 1339.
(16) Desfrançois, C. *Phys. Rev. A* **1995**, *51*, 3667.
(17) Gutowski, M.; Skurski, P.; Jordan, K. D.; Simons, J. *Int. J. Quantum Chem.* **1997**, *64*, 183.
(18) Smith, D. M. A.; Smets, J.; Elkadi, L.; Adamowicz, L. *Chem. Phys. Lett.* **1999**, *305*, 169.
(19) Périquet, V.; Moreau, A.; Carles, S.; Schermann, J. P.; Desfrançois, C. *J. Electron Spectrosc. Relat. Phenom.* **2000**, *106*, 141.
(20) Kwon, O. Y.; Kim, S. Y.; No, K. T.; Jhon, M. S.; Scheraga, H. A. *J. Phys. Chem.* **1996**, *100*, 17670.
(21) Desfrançois, C. To be published.
(22) Zeiri, Y. *Phys. Rev. E* **1995**, *51*, 2769.
(23) Wales, D. J.; Scheraga, H. A. *Science* **1999**, *285*, 1368.
(24) Adamowicz, L. Private communication.
(25) Kim, N. J.; Kang, H. K.; Jeong, G.; Kim, Y. S.; Lee, K. T.; Kim, S. K. *J. Phys. Chem. A* **2000**, in press.
(26) Martopraviro, M. A.; Backsay, G. B. *Mol. Phys.* **1995**, *573*, 573.
(27) Bael, M. K. V.; Smets, J.; Schoone, K.; Houben, L.; McCarthy, W.; Adamowicz, L.; Nowak, M. J.; Maes, G. *J. Phys. Chem.* **1997**, *101*, 2397.
(28) Djafari, S.; Lembach, G.; Barth, H. D.; Brutschy, B. *Z. Phys. Chem.* **1996**, *195*, 253.
(29) Lide, D. R. *CRC Handbook of Chemistry and Physics*; CRC Press: Boca Raton, FL, 1995.
(30) Basch, H.; Garmer, D. R.; Jasien, P. G.; Krauss, M.; Stevens, W. J. *Chem. Phys. Lett.* **1989**, *163*, 514.